Plasmas. New York: McGraw-Hill, 1969.
[4] A. V. Vashkovskii *et al.*, "Interaction of surface magnetostatic waves with carriers on a ferrite-semiconductor interface," *Sov. Phys.—JETP Lett.*, vol. 16, p. 4, 1972.
[5] G. A. Benett and J. D. Adam, "Identification of surface wave resonances on a metal backed YIG slab," *Electron. Lett.*, vol. 6, p. 789, 1970.
[6] R. J. Briggs, *Electron-Stream Interaction with Plasmas*. Cambridge, Mass.: M.I.T. Press, 1964.
[7] K. Ohtsuki *et al.*, private communication.
[8] J. D. Adam, "Delay of magnetostatic surface waves in YIG," *Electron. Lett.*, vol. 6, p. 718, 1970.
[9] R. E. de Wames and T. Wolfram, "Characteristics of magnetostatic surface waves for a metalized ferrite slab," *J. Appl. Phys.*, vol. 41, p. 5243, 1970.
[10] K. Kawasaki and M. Umeno, "Influence of surface metallization on the propagation characteristics of surface magnetostatic waves in an axially magnetized rectangular YIG rod," *IEEE Trans. Microwave Theory Tech.*, vol. MTT-22, pp. 391–394, Apr. 1974.
[11] H. Van de Vaart, "Influence of metal plate on the surface magnetostatic modes of magnetic slab," *Electron. Lett.*, vol. 6, p. 601, 1970.
[12] K. Kawasaki, H. Takagi, and M. Umeno, "Passband control of surface magnetostatic waves by spacing a metal plate apart from the ferrite surface," this issue, pp. 924–929.

Passband Control of Surface Magnetostatic Waves by Spacing a Metal Plate Apart from the Ferrite Surface

KIYOHIRO KAWASAKI, HIROTAKA TAKAGI, AND MASAYOSHI UMENO, MEMBER, IEEE

Abstract—**The effect of a metal plate on the propagation characteristics of surface magnetostatic waves (SMW) propagating perpendicular to an external dc magnetic field was studied by varying the spacing of the metal plate from the ferrite surface. Continuous passband control is obtained by changing the spacing from zero to infinity and the existence of a partial stopband for the interchange of the input and output ports is also obtained in addition to the disappearance of nonreciprocal propagation for a finite spacing of the metal plate.**

INTRODUCTION

MUCH EFFORT has recently been devoted to the study of surface magnetostatic waves (SMW) with the development of magnetic thin films of high quality. SMW propagating perpendicular to an external dc magnetic field have strong nonreciprocity depending on the direction of propagation. SMW which propagate along the metal-bounded surface and along the free surface are known as a ferrite-metal (FM) and as a ferrite-air (FA) mode, and their passbands are from

$$\omega = [\omega_0(\omega_0 + \omega_M)]^{1/2} \quad \text{to} \quad \omega = \omega_0 + \omega_M$$

and from $\omega = [\omega_0(\omega_0 + \omega_M)]^{1/2}$ to $\omega = \omega_0 + \omega_M/2$, respectively, where $\omega_0 = \gamma H_0$ is the precession angular frequency and $\omega_M = \gamma 4\pi M$ is the angular frequency of the saturation magnetization. Nonreciprocity of the waves can be used in the application to microwave components [1]–[3].

Van de Vaart has derived the dispersion relations for SMW propagating in a ferrite slab with a conductive plate located at a small distance parallel to the surface of the slab. SMW propagating along the metal-bounded surface in this configuration consist of forward or backward waves depending on the wavelength of the mode and the distance of the conducting plate from the ferrite surface [4]. Bongianni has also derived the same dispersion relations and performed some experiments with a dielectric-layered structure consisting of an epitaxial YIG film separated by a thin dielectric layer. He has reported experimental results mainly concerning the delay characteristics of the waves [5]. The dependence of the waves on the direction of the external dc magnetic field was first introduced by Sparks, and the theoretical results agreed surprisingly well with the Brundle and Freedman experimental values [6], [7].

In a previous paper, we have reported the influence of metal plates on the propagation characteristics of SMW propagating in the direction of the external dc magnetic field, and then proposed a new type of microwave filter which is mechanically tunable [8].

In this paper, we show the continuous passband control of SMW propagating perpendicular to the external dc magnetic field by changing the spacing of the metal plate from the ferrite surface. The same phenomenon occurs for SMW propagating in the direction of the external dc magnetic field. The difference between the two cases is an asymmetrical situation for the metal plate located parallel to the ferrite surface for the former and a symmetrical situation for the metal plates placed parallel to the surfaces for the latter. We show additional features of the waves: the disappearance of nonreciprocity for a finite spacing of the metal plate and the existence of a

Manuscript received March 18, 1974; revised June 26, 1974.
The authors are with the Department of Electronics, Nagoya University, Nagoya, Japan.

partial stopband for the interchange of the input and output ports. Experimental results obtained at S and X bands agree well with theoretical estimates.

THEORY

Following Young's model, let the YIG slab be placed between two semi-infinite metal walls, with a metallic boundary situated at a small distance from one of its base planes, as shown in Fig. 1. The waves propagate along the $\pm y$ directions and the external dc magnetic field is along the z direction. The magnetic field is expressed as $\boldsymbol{H} = \nabla\Phi$ from the magnetostatic approximation $\nabla \times \boldsymbol{H} = 0$. The magnetic potential inside and outside the slab may be expressed as

$$\Phi_1 = (A_1 \cos \alpha x + B_1 \sin \alpha x) \cdot \cos \beta z \cdot \exp\,(i(\omega t \mp ky)), \quad 0 < x < a \tag{1}$$

$$\Phi_2 = A_2 \cdot \exp\,(-\gamma x) \cdot \cos \beta z \cdot \exp\,(i(\omega t \mp ky)), \quad a < x \tag{2}$$

$$\Phi_3 = (A_3 \cosh \gamma x + B_3 \sinh \gamma x) \cdot \cos \beta z \cdot \exp\,(i(\omega t \mp ky)), \quad -c < x < 0. \tag{3}$$

From Maxwell's equation $\nabla \times \boldsymbol{B} = 0$, the characteristic equations are given as follows:

$$\mu(\alpha^2 + k^2) + \beta^2 = 0 \tag{4}$$

$$\gamma^2 - k^2 - \beta^2 = 0. \tag{5}$$

Following (5), γ must be real for the guided magnetostatic waves since the propagating modes are given for real values of k and β. Magnetostatic waves which have their energy density distributed throughout the sample are volume magnetostatic waves (VMW) and α^2 is positive. Magnetostatic waves whose energy density concentration occurs near the surface are SMW and α^2 must be negative: $-\alpha^2 = X^2 > 0$. The boundary conditions are such that the normal component of the magnetic flux density must vanish on the metal surface at $x = -c$ and the normal components of the magnetic flux density and the tangential components of the magnetic field must be continuous on the slab surfaces at $x = 0$ and $x = a$. From these boundary conditions, a transcendental equation for X is obtained

$$\mu\gamma X \cdot (\tanh \gamma c + 1) \cdot \cosh Xa + \{\gamma^2 \tanh \gamma c \mp \kappa\gamma k(1 - \tanh \gamma c) - \kappa^2 k^2 + \mu^2 X^2\} \cdot \sinh Xa = 0. \tag{6}$$

Equations (4)–(6) give the dispersion relations of SMW. In (4)–(6), μ and κ are the diagonal and off-diagonal components of the permeability tensor and $\beta = n\pi/b$, where b is the slab width and n is a positive integer. To examine the effect of the spacing of the metal plate, let $c \to \infty$ in (6). Then the following expression:

$$2\mu\gamma X \cdot \cosh Xa + (\gamma^2 - \kappa^2 k^2 + \mu^2 X^2) \cdot \sinh Xa = 0 \tag{7}$$

is obtained. And let $c \to 0$, then

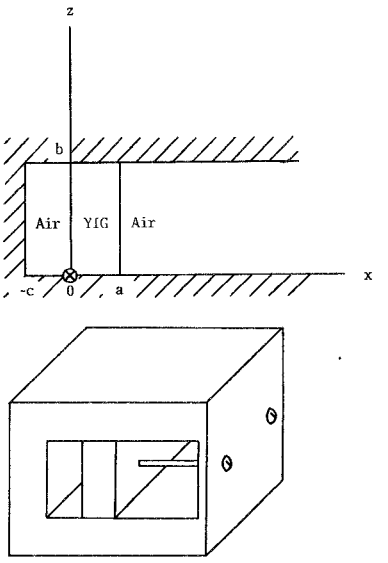

Fig. 1. Coordinate system and a schematic drawing of a sample holder. $a = 0.55$ mm, $b = 2.7$ mm.

$$\mu\gamma X \cdot \cosh Xa - (\kappa^2 k^2 - \mu^2 X^2 \pm \kappa\gamma k) \cdot \sinh Xa = 0 \tag{8}$$

is obtained. In (8) the upper sign refers to the waves propagating in the $+y$ direction along the $x = a$ surface and the lower sign to the waves propagating in the $-y$ direction along the $x = 0$ surface, and are known as FA and FM modes, respectively [1]–[3]. From symmetrical properties of propagation, it is clear that the nonreciprocity of the waves appears depending on the direction of propagation for $c = 0$ and does not appear for $c = \infty$. The passbands of the waves are obtained by letting $k \to 0$ and does not appear for $c = \infty$. The passbands of the waves are obtained by letting $k \to 0$ and $\beta \to 0$, and $k \to \infty$ in (7) and (8). For $c = \infty$

$$[\omega_0(\omega_0 + \omega_M)]^{1/2} < \omega < \omega_0 + \omega_M/2 \tag{9}$$

and for $c = 0$

$$[\omega_0(\omega_0 + \omega_M)]^{1/2} < \omega < \omega_0 + \omega_M/2, \quad \text{for FA mode} \tag{10}$$

$$[\omega_0(\omega_0 + \omega_M)]^{1/2} < \omega < \omega_0 + \omega_M, \quad \text{for FM mode.} \tag{11}$$

For a finite value of the spacing, it is assumed that the slab thickness is much longer than the wavelength: $ka \gg 1$, then (6) becomes as follows:

$$\mu\gamma X \cdot (\tanh \gamma c + 1) + \gamma^2 \tanh \gamma c \mp \kappa\gamma k \cdot (1 - \tanh \gamma c) - \kappa^2 k^2 + \mu^2 X^2 = 0. \tag{12}$$

For the waves of short wavelength, (12) is further simplified as follows:

$$(1 + \mu \pm \kappa) \cdot \{\tanh kc + (\mu \mp \kappa)\} = 0. \tag{13}$$

For the $+y$-directed waves along the $x = a$ surface, the first factor in (13) yields the resonant frequency

$$\omega = \omega_0 + \omega_M/2. \tag{14}$$

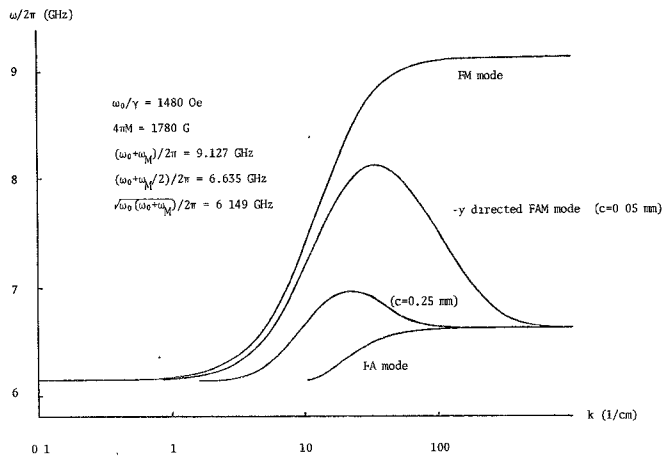

Fig. 2. Dispersion relations of surface magnetostatic waves for $n = 1$ modes.

For the $-y$-directed waves along the $x = 0$ surface, the second factor in (13) yields the dispersion relation

$$\omega = \omega_0 + \frac{\omega_M}{1 + \tanh kc}. \tag{15}$$

For small values of k, ω approaches $\omega_0 + \omega_M$; we have the same situation as if c is small. For large values of k, ω approaches $\omega_0 + \omega_M/2$; we have the same situation as if the conducting plate is far apart from the ferrite surface. The waves given by (15) are backward waves, similar to the magnetostatic waves propagating in the direction of the external dc magnetic field [4]. Note that (12)–(15) are derived under the assumption of $ka \gg 1$.

The computer-aided result of the complete spectrum of wavenumber k for a finite value of the spacing c given by (6) is shown in Fig. 2. The z dependence of the waves is given by $k_z = \beta = n\pi/b$ with $n = 1$. For the waves propagating in the $-y$ direction there exist a point where the waves change from forward waves to backward waves as the wavenumber k increases. Increase of the spacing brings about the passband narrowing of the waves, and the passband coincides with that of the FA mode in the limit of $c \to \infty$. For the waves propagating in the $+y$ direction, the energy density of the waves is largest at the $x = a$ surface and the effect of the metal plate is very weak, and the spectrum is essentially the same as the FA mode. The fundamental nature of the waves in this configuration is the same for the $n = 0$ mode. The dependence of the waves on the direction of the external dc magnetic field brings about the cutoff wavenumber and also effects significantly the exponential decay rate of the waves for long wavelengths.

EXPERIMENTAL PROCEDURES

Our sample was a single crystal of YIG with saturation magnetization of 1780 G and linewidth below 0.5 Oe. It had dimensions of $0.55 \times 2.7 \times 10.0$ mm^3 and the surfaces along which SMW propagate were polished optically flat. Microwave power from a klystron was applied to a thin wire antenna near the slab end. The detection antenna was located near the opposite end of the slab. These antennas were parallel to the direction of the external dc magnetic field.

The driving power was limited to less than 0.1 mW to avoid saturation effects and instabilities since the energy density of the surface waves was quite high at the surfaces [9]. In our experiments, saturation of transmitted power and widening of the resonance linewidth were observed when the applied microwave power exceeded 1 mW. Resonance absorptions of VMW were observed for the application of microwave power above 1 mW and the saturation of transmitted power did not occur until the applied microwave power exceeded 10 mW. These facts may be caused by a high saturation level of VMW in addition to the weak excitation for VMW with the above-mentioned arrangement of the antenna.

Transmitted power or reflected power from a circulator was rectified by a diode 1N23B and applied to a Y input of an X–Y recorder. The X input was the sweep voltage for the dc magnetic field. We have determined the modes of propagating magnetostatic waves from the spectrum of the transmitted or reflected power versus internal dc magnetic-field strength. For SMW various resonance absorptions were obtained for the choice of the spacing of the metal plate from the ferrite surface. On the contrary, resonance absorptions of VMW were not significantly influenced by the change of the spacing.

Pulse-modulated microwave power with a p-i-n diode switch was applied for the measurement of delay characteristics. The pulse had a width of 0.2 μs. Delayed signals were mixed with a local oscillation signal, amplified, detected, and displayed on an oscilloscope.

The spacing of the metal plate from the ferrite surface was changed by a suitable combination of Teflon films of 0.05-, 0.1-, 0.15-, 0.2-, and 0.25-mm thicknesses with small tan δ. Teflon films and the YIG plate were slightly pressed onto the base metallic plate by two thin Teflon screws in order to obtain uniform contacts in the boundary planes.

EXPERIMENTAL RESULTS AND DISCUSSION

In Fig. 3 the differences of transmitted powers are shown for the $\pm y$-directed SMW with and without the spacing. The horizontal axis denotes the external dc magnetic-field strength H_E and the vertical axis denotes the detected voltage of the transmitted power. The resonance absorptions of VMW occurred at external dc magnetic-field strengths above 1050 Oe and the amplitudes were small compared with those of SMW because the excitation was weak for VMW. The resonance absorptions of VMW are not identified in the figures. The positions and the field range of the resonance absorptions of VMW were not significantly influenced by the spacing of the metal plate from the ferrite surface.

Time delays of SMW were observed just below the cutoff point H_p of the FA mode. The attenuation rate per unit delay time was $50 \sim 60$ dB/μs, and the maximum delay time was 0.4 μs for SMW, which means that the propagation loss is larger than the values of $15 \sim 20$ dB/μs ob-

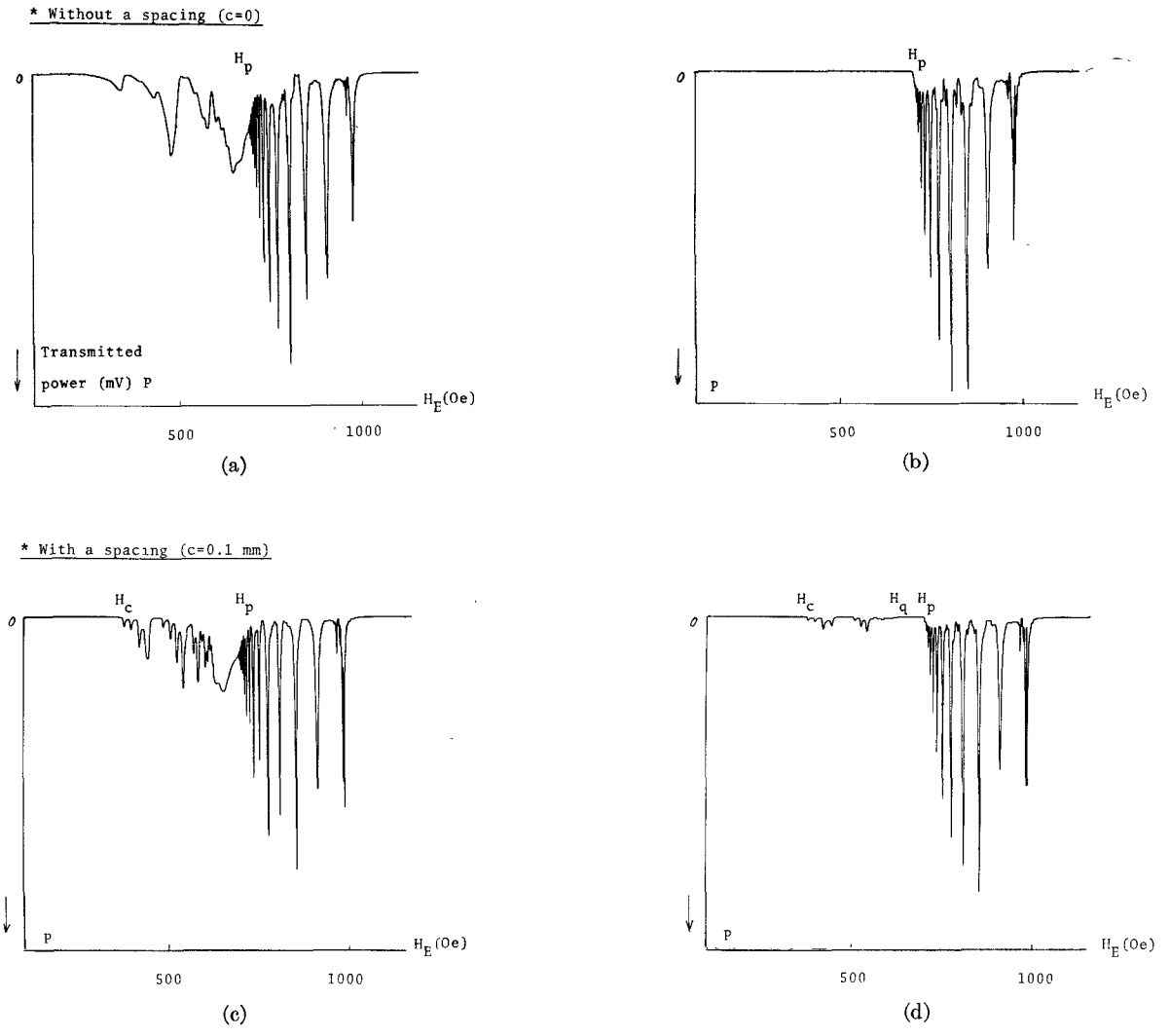

Fig. 3. Examples of transmitted microwave power as a function of the external dc magnetic-field strength H_E. Frequency: $\omega/2\pi = 4.143$ GHz. The horizontal axis is a linear scale and the full scale is 90 mV. (a) and (c) Propagation in the $-y$ direction. (b) and (d) Propagation in the $+y$ direction.

served for VMW. For the $+y$-directed SMIW only the delays of the FA modes were observed. For the $-y$-directed SMW time delays of the FA modes with very small amplitudes were observed accompanying zero delays of the FM or ferrite–air–metal (FAM) modes with large amplitudes. Waveforms of the delayed signals were distorted by the application of microwave power above 1.0 mW, which indicates a low saturation level of SMW. The effect of the spacing on the delay time was almost not observed for the material parameter used in our experiments. Detailed examination of the dispersion relations reveals that the FA modes have larger wavenumbers and faster group velocities with increasing spacing. These natures should be remarkable for the thinner YIG slab than the present one, as Bongianni has shown in his computer-aided results with an epitaxial YIG film [5].

The broad transmission band below H_p in Fig. 3(a) is due to the FM mode only. Resonance absorptions of the FM mode were strongly influenced by the small spacing between the ferrite surface and the base metallic plate, and the positions of them varied significantly by loosening the pressure with Teflon screws. Resonance absorptions occurring above H_p are caused by the round-trip propagation of the $+y$-directed FA mode and the $-y$-directed FM mode; since the internal dc magnetic field H_0 satisfies $(\omega - \omega_M/2)/\gamma < H_0 < [-\omega_M + (\omega_M^2 + 4\omega^2)^{1/2}]/2\gamma$, both modes can propagate and the resonance absorptions occur at the same dc magnetic field for the $\pm y$-directed SMW. The resonance condition is thus expressed as

$$(k_{FA} + k_{FM}) \cdot L = 2N\pi, \qquad N: \text{positive integer} \quad (16)$$

where L is the length of the slab along the direction of propagation. In Fig. 4 the values of N obtained theoretically from (8) and (16) and those observed experimentally are shown. Agreement with theory is remarkably good although the demagnetizing field is not taken into account. The same results have been reported by Benett *et al.* [10]. As may be seen from Fig. 3(a) and (b), nonreciprocal

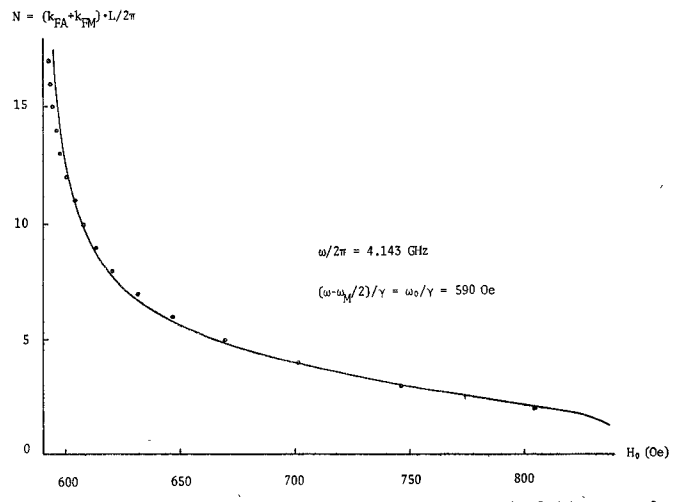

Fig. 4. Peak number N versus internal dc magnetic-field strength. Theoretical curve is for the $n = 1$ mode (solid line) and experimental resonance peaks (open circle).

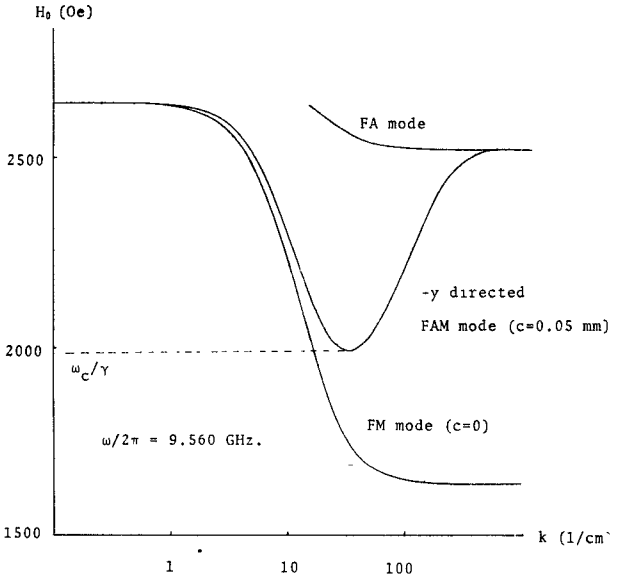

Fig. 5. Dispersion relations of surface magnetostatic waves for $n = 1$ modes as a function of the internal dc magnetic-field strength.

transmission of SMW is observed depending on the direction of propagation.

The upper limit of the passband of the FAM mode changes from $\omega = \omega_0 + \omega_M$ to $\omega = \omega_0 + \omega_M/2$ as the spacing varies from zero to infinity. Hence the passband of the FAM mode can be chosen freely in the above range by changing the spacing. The magnetic-field strength H_c in Fig. 3(c) and (d) corresponds to the cutoff magnetic-field strength ω_c/γ in Fig. 5, where the dispersion relations of SMW are shown as a function of the internal dc magnetic-field strength. In Fig. 6 the cutoff dc magnetic-field strength H_c is shown as a function of the spacing c. Experimental values of H_c were measured from the cutoff magnetic field H_p on the spectrum to avoid the effects of the demagnetizing and anisotropy fields. In Fig. 6(a) experimental results obtained at S band of 4.143 GHz and the theoretical curve are shown. The theoretical curve is given for the $n = 1$ mode. The lower cutoff dc magnetic-field strength for the FM mode ($c = 0$) is negative at S band. The departures from the theoretical curve at low dc fields may be due to lack of saturation of magnetization. To avoid the unsaturation of magnetization, experiments were performed also at X band and the results at 9.560 GHz are shown in Fig. 6(b). The departure from the theoretical curve for the FM mode may be due to the large conversion loss which is brought about by the conduction mechanism at the metal surface and the short wavelength of the mode. Here again agreement with theory is good when the z dependence of the waves is given by $k_z = n\pi/b$ with $n = 1$.

Comparing Fig. 3(c) and (d), there exists a transmission band below H_p and the nonreciprocity of the waves disappears. This fact is explained as follows. The FAM modes with a finite spacing are backward waves for large k and the direction of the phase velocity is opposite to that of the group velocity as may be seen from Fig. 2. There exist two values of k which satisfy the dispersion relations for the range of the internal dc magnetic-field strength $\omega_c/\gamma < H_0 < (\omega - \omega_M/2)/\gamma$. The nonreciprocal property

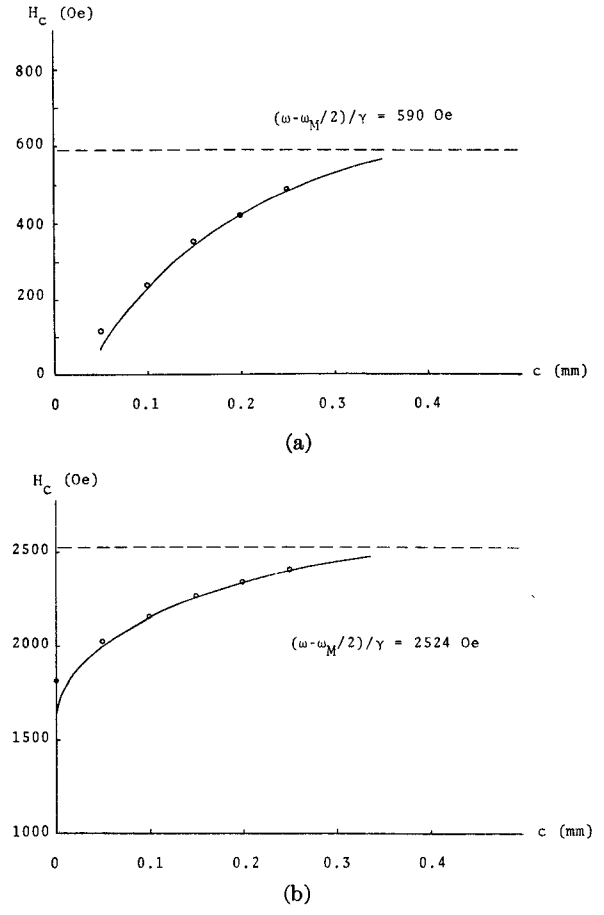

Fig. 6. Cutoff dc magnetic-field strength H_c of $n = 1$ FAM and FM modes as a function of the spacing c. Theoretical value (solid line); experimental value (open circle). (a) $\omega/2\pi = 4.143$ GHz. (b) $\omega/2\pi = 9.560$ GHz.

disappears since the direction of the group velocity of the forward k_1 mode is toward the $-y$ direction and that of the backward k_2 mode toward the $+y$ direction. Resonance absorptions occurring above H_p are located at the same

position due to the round-trip propagation of the FA and the FAM modes.

Time delays of the FAM mode should be expected to occur at H_c. But the change of the group velocity is quite sharp near H_c compared with the change near H_p as may be seen from Fig. 5. Amplified transmitted power showed a sudden jump in the spectrum and a sudden appearance on an oscilloscope if the external dc magnetic field was slowly swept with time. To observe the time delays of the FAM mode, much greater stability of frequency and dc magnetic field is required than is presently available.

A partial stopband for the $+y$-directed FAM mode is observed from H_q to H_p, while it is replaced by a continuous passband from H_c to H_p for the $-y$-directed FAM mode as shown in Fig. 3(c) and (d). This fact is explained as follows. The internal dc magnetic-field strength is lower at the center than at the ends of the slab by about 100 Oe for our sample. Thus the distributions of wavelength for the k_1 and the k_2 modes are opposite. The wavelength becomes longer for the k_1 mode and shorter for the k_2 mode with increasing internal dc magnetic field. If the internal dc magnetic-field strength exceeds $(\omega - \omega_M/2)/\gamma$, the k_2 mode becomes cutoff. Even if the internal dc magnetic-field strength does not exceed $(\omega - \omega_M/2)/\gamma$, the wavelength of the k_2 mode is short at the slab ends near the excitation and the detection antennas, and so the conversion loss from microwave to the k_2 mode is quite large. On the other hand, the k_1 mode is within a passband and the wavelength is long even if the k_2 mode is cutoff. Hence the conversion loss from microwave to the k_1 mode is small and the propagation of the k_1 mode is allowed with a small transmission loss. Following the above-mentioned principle, when the internal dc magnetic-field strength is somewhat below the cutoff field of the FA mode: $H_0 < (\omega - \omega_M/2)/\gamma$, nonreciprocal propagation is obtained. The strength of the cutoff field H_c varies as a function of the spacing and so the strength of H_q above which the k_2 mode cannot propagate with a small transmission loss also varies. In Fig. 7, the change of the magnetic-field strength of H_q is shown as a function of the spacing. A partial stopband also narrows with increasing spacing.

CONCLUSION

The effect of a metal plate on the propagation characteristics of SMW was studied by changing the distance between the ferrite surface and the metal plate. It was concluded that the upper limit of the passband of SMW propagating along the ferrite surface varies continuously from $\omega = \omega_0 + \omega_M$ to $\omega = \omega_0 + \omega_M/2$ as the spacing of the metal plate from the ferrite surface varies from zero to infinity. The following additional features are experimentally shown: the disappearance of the nonreciprocity of the waves for a finite spacing and the existence of a partial stopband for the interchange of the input and the output ports.

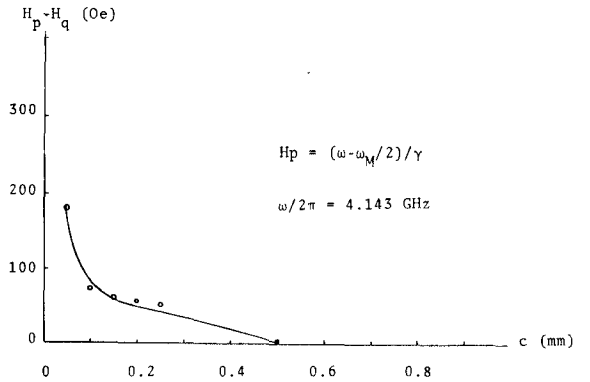

Fig. 7. Cutoff dc magnetic-field strength H_q of stopband as a function of the spacing c. Experimental value (open circle).

By choosing a suitable spacing of the metal plate, the passband of SMW can be controlled and a broad transmission can be obtained by exciting the multiple modes (lowest mode plus higher order modes) [11].

REFERENCES

[1] P. Young, "Effect of boundary conditions on the propagation of surface magnetostatic waves in a transversely magnetized thin YIG slab," *Electron. Lett.*, vol. 5, p. 429, 1969.
[2] J. D. Adam, G. A. Benett, and J. Wilkinson, "Experimental observation of magnetostatic modes in a YIG slab," *Electron. Lett.*, vol. 6, p. 434, 1970.
[3] S. R. Sashadri, "Surface magnetostatic modes of a ferrite slab," *Proc. IEEE* (Lett.), vol. 58, pp. 506–507, Mar. 1970.
[4] H. Van de Vaart, "Influence of metal plate on the surface magnetostatic modes of magnetic slab," *Electron. Lett.*, vol. 6, p. 601, 1970.
[5] W. L. Bongianni, "Magnetostatic propagation in a dielectric layered structure," *J. Appl. Phys.*, vol. 43, p. 2541, 1972.
[6] L. K. Brundle and N. J. Freedman, "Magnetostatic surface waves on a YIG slab," *Electron. Lett.*, vol. 4, p. 132, 1968.
[7] M. Sparks, "Magnetostatic surface modes of a YIG slab," *Electron. Lett.*, vol. 5, p. 618, 1969.
[8] K. Kawasaki and M. Umeno, "Influence of surface metallization on the propagation characteristics of surface magnetostatic waves in an axially magnetized rectangular YIG rod," *IEEE Trans. Microwave Theory Tech.*, vol. MTT-22, pp. 391–394, Apr. 1974.
[9] J. D. Adam, "Delay of magnetostatic surface waves in YIG," *Electron Lett.*, vol. 6, p. 718, 1970.
[10] G. A. Benett and J. D. Adam, "Identification of surface wave resonances on a metal backed YIG slab," *Electron. Lett.*, vol. 6, p. 789, 1970.
[11] F. A. Olson *et al.*, "Propagation of magnetostatic surface waves in YIG rods," *J. Appl. Phys.*, vol. 38, p. 1218, 1967.